Microwave Generation by P2 Dynamics of Optically Injected Semiconductor Laser

Xiaoyue Yu, Fangzheng Zhang, *Senior Member, IEEE*, Xin Yan, Gengze Wu, Xinyao Han, *Student Member, IEEE*, Shilong Pan, *Fellow, IEEE*, and Kai Wang

***Abstract*—In this paper, an approach for photonic generation of microwave signals by period-two (P2) dynamics in an optically injected semiconductor laser is investigated, which provides a supplementary method for generating microwave signals below the period-one (P1) oscillation frequencies. The characteristics of P2 oscillation including the frequency tunability and frequency-switching time are numerically investigated, which shows the potential of microwave signal generation by P2 dynamics. In the experiment, the generation of single-frequency and stepped-frequency (SF) microwave signals based on P2 dynamics are demonstrated. For single-frequency signal generation, optical injection combined with dual-loop optoelectronic feedback is achieved to suppress the phase noise. In the experiment, single-frequency signals with adjustable frequencies from 1.72 GHz to 8.68 GHz are generated with the phase noise lower than −118.54 dBc/Hz @10kHz and the side-mode suppression ratio (SMSR) ratio over 69.8 dB. For SF microwave signal generation, a 3-GHz (3-6 GHz) bandwidth signal with multiple discrete frequencies is generated of which the frequency stability and accuracy are improved the by incorporating single-loop optoelectronic feedback. The results validate the feasibility of microwave signal generation by P2-dyanmics, which can be applied in wireless communication and radar systems.**

***Index Terms*—Laser dynamics, microwave photonics, microwave signal generation, optical injection, semiconductor lasers.**

I. Introduction

NONLINEAR dynamics of semiconductor lasers have been extensively studied within the recent decades. These nonlinear laser dynamics can be easily excited by various means including optical feedback [1], [2], [3], optical injection [4], [5], [6], and optoelectronic feedback [7], [8], [9], wherein the laser dynamics excited by optical injection have attracted much attention owing to their simple structure and superior frequency tunability. Generally speaking, an optically injected semiconductor laser usually follows a period-doubling route to chaos, including stable locking, chaos, period-one (P1) oscillation, period-two (P2) oscillation, quasi-periodic oscillation and so on [7]. The stable locking has been applied for modulation bandwidth enhancement, wavelength synchronization and laser coherence enhancement [10], [11], [12]. Chaos state are widely applied in secure communication, optical reflectometry, chaotic radar and high-speed random bit generation [13], [14]. Periodic oscillations exhibiting a characteristic of self-sustained microwave oscillation with asymmetric single sideband modulation are usually used for generation of microwave signals [15], [16], [17], [18], [19]. In recent years, various microwave signal generation schemes by P1 dynamics of optically injected semiconductor laser have been proposed and demonstrated [20], [21], [22], [23], [24], [25], [26], [27]. When P1 oscillation is excited, oscillation sidebands in the cavity of laser are emerged and equally separated from the regenerated carrier, which leads to the enhanced modulation characteristics of an injection-locked oscillator. Benefiting from the bandwidth enhancement effect, the P1 oscillation frequency varies approximately linearly with the injection strength, through which microwave signals can be generated with frequencies up to 100 GHz [18], [28]. Compared with the other microwave photonic signal generation systems realized by heterodyne-beating [29], direct modulation [30], space-to-time mapping [31], or frequency-to-time mapping [32], microwave signal generation by P1 dynamics in an optically injected semiconductor laser features a compact structure and good frequency tunability. However, since the wavelength of the semiconductor laser after optical injection is significantly red-shifted relative to the free-running wavelength, it is difficult to exit P1 oscillation with frequency lower than the relaxation oscillation frequency (usually at ∼10 GHz) of the injected laser even at small detuning frequency. To solve this problem, P2 oscillation excited in an optically injected semiconductor laser provides an effective method to extend the microwave signal generation towards the frequency bands lower than 10 GHz. As the injection strength increases, the semiconductor laser under optical injection is oscillated at a fundamental frequency and undergoes period doubling oscillation bifurcation. When P2 oscillation is excited, the subharmonic frequency at half of the fundamental microwave frequency appears, resulting in microwave frequency division [33]. Thus, P2 oscillation yielding

Received 12 December 2024; revised 5 February 2025; accepted 9 February 2025. Date of publication 13 February 2025; date of current version 16 May 2025. This work was supported in part by the National Key Research and Development Program of China under Grant 2021YFB2800803, in part by the National Natural Science Foundation of China under Grant 62371224, in part by the Natural Science Foundation of Jiangsu Province under Grant BK20221479, and in part by the Fundamental Research Program for Young Student of National Key Laboratory of Microwave Photonics under Grant 24-JSKY-ZZKT-QNXS-01. *(Corresponding author: Fangzheng Zhang.)*

Xiaoyue Yu, Fangzheng Zhang, Xin Yan, Gengze Wu, Xinyao Han, and Shilong Pan are with the National Key Laboratory of Microwave Photonics, Nanjing University of Aeronautics and Astronautics, Nanjing 210016, China (e-mail: zhangfangzheng@nuaa.edu.cn).

Kai Wang is with the China Electronics Technology Group Corporation No.38 Research Institute, Hefei 230088, China.

Color versions of one or more figures in this article are available at https://doi.org/10.1109/JLT.2025.3541204.

Digital Object Identifier 10.1109/JLT.2025.3541204

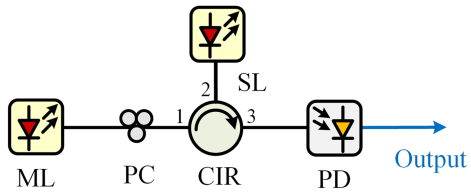

Fig. 1. Typical schematic setup of the optically injected semiconductor laser system. ML, master laser; SL, slave laser; PC, polarization controller; CIR, optical circulator; PD, photodetector.

TABLE I
PARAMETERS IN THE SIMULATION

Parameter	Symbol	Value
Differential carrier relaxation rate	γ_n	7.53×10^9 s^{-1}
Cavity decay rate	γ_c	5.36×10^{11} s^{-1}
Nonlinear carrier relaxation rate	γ_p	1.91×10^{10} s^{-1}
Spontaneous carrier relaxation rate	γ_s	5.96×10^9 s^{-1}
Linewidth enhancement factor	b	3.2
Normalized bias current density	$\tilde{J}$	1.222
Injection strength	ξ	Variable
Detuning frequency	f_i	Variable

subharmonic frequency provides the possibility of microwave signal generation in low frequency band. However, to the best of our knowledge, the research of P2 oscillation is still stays in the theoretical stage. The generation of microwave signals by the P2 dynamics has yet to be explored.

In this paper, microwave signal generation by P2 dynamics of an optically injected semiconductor laser is demonstrated through both numerical simulation and experiment. First, the characteristic of P2 oscillation subject to optical injection is studied numerically, in which the frequency tunability and frequency-switching time of P2 oscillation are analyzed. Then, an experiment is conducted to generate single-frequency and stepped-frequency (SF) microwave signals. Thereinto, to reduce the linewidth and improve the side-mode suppression ratio (SMSR) of the single-frequency signal, a optoelectronic feedback dual-loop structure is applied to the optical injection system. In the experiment, single-frequency microwave signals with tunable frequencies from 1.72 GHz to 8.68 GHz is generated, of which the SMSR is measured at 69.8 dB and the phase noise is kept below −118 dBc/Hz at 10 kHz offset and −134.20 dBc/Hz at 100 kHz offset. In addition, a SF microwave signals with multiple discrete frequencies in the range from 3 GHz to 6 GHz is also generated, of which the bandwidth and frequency-step can be controlled by changing the injection parameters. By using single-loop optoelectronic feedback, the frequency accuracy and stability of the generated SF signal are significantly improved. These results verify that P2 oscillation can be used as a complement of P1 oscillation for photonic generation of low frequency microwave signals.

II. Numerical Analysis

The typical schematic setup of the optically injected semiconductor laser system is illustrated in Fig. 1. A continues wave light from the master laser (ML) is injected into a slave laser (SL) via an optical circulator (CIR). To maximize the injection efficiency, a polarization controller (PC) before the CIR is utilized to align the polarization of the ML with that of the SL. By properly altering the injected optical power and frequency, different nonlinear dynamics can be invoked in the SL. By sending the optical signal of the SL into a photodetector (PD) for optical-to-electrical conversion, microwave signals can be generated.

To explore the performance of P2 oscillation, numerical calculations under optical injection are conducted by solving the normalized laser nonlinear rate equations [4]:

$$\frac{da_r}{dt} = \frac{1}{2}\left[\frac{\gamma_n\gamma_c}{\gamma_s\tilde{J}}\tilde{n} - \gamma_p(a_r^2+a_i^2-1)\right](a_r+ba_i) + \xi\gamma_c\cos(2\pi f_i t) \quad (1)$$

$$\frac{da_i}{dt} = \frac{1}{2}\left[\frac{\gamma_n\gamma_c}{\gamma_s\tilde{J}}\tilde{n} - \gamma_p(a_r^2+a_i^2-1)\right](-ba_r+a_i) - \xi\gamma_c sin(2\pi f_i t) \quad (2)$$

$$\frac{d\tilde{n}}{dt} = -\gamma_s\tilde{n} - \gamma_n(a_r^2+a_i^2)\tilde{n} - \gamma_s\tilde{J}(a_r^2+a_i^2-1) + \frac{\gamma_s\gamma_p}{\gamma_c}\tilde{J}(a_r^2+a_i^2)(a_r^2+a_i^2-1) \quad (3)$$

where a_r and a_i are the real and imaginary parts of the normalized complex intracavity photon amplitude of the SL at the oscillating frequency. $\tilde{n}$ is the corresponding normalized carrier density. $\tilde{J}$ is the normalized bias current density above laser threshold. The laser intrinsic parameters of differential carrier relaxation rate, cavity decay rate, nonlinear carrier relaxation rate, spontaneous carrier relaxation rate, and linewidth enhancement factor are denoted by γ_n, γ_c, γ_p γ_s, and b, respectively. In addition, ξ is the injection strength which is defined as the amplitude ratio between the injected light from ML and free-running SL. The detuning frequency f_i is the frequency difference between the ML and free-running SL [20]. In the simulation, the intrinsic parameters of the lasers are chosen as those in [15], which are listed in Table I. In this case, the corresponding relaxation oscillation frequency of the SL at free-running condition is given by $f_r = (\gamma_c\gamma_n+\gamma_s\gamma_p)^{1/2}/2\pi$=10.25 GHz. In the simulation, the fourth-order Runge-Kutta integration is conducted with a temporal step of 0.25 ps within a duration period of 0.1 μs.

Fig. 2 shows the numerally calculated nonlinear dynamics mapping of an optically injected semiconductor laser as a function of the injection strength ξ and the detuning frequency f_i. Especially, the regions for period oscillations with periods greater than two in Fig. 2 are marked as PN. In Fig. 2, a large region of stable locking states is observed, which is bounded by the Hopf-bifurcation line. As the detuning frequency increases, a large region of P1 oscillation states is designated above the stable locking region. Additionally, the P1 oscillation states also can be observed at low injection strength levels with negative detuning frequency. The regions of P2 oscillation, PN oscillation and chaos are embedded within the P1 oscillation state region, where the detuning frequency f_i is close to the free-running

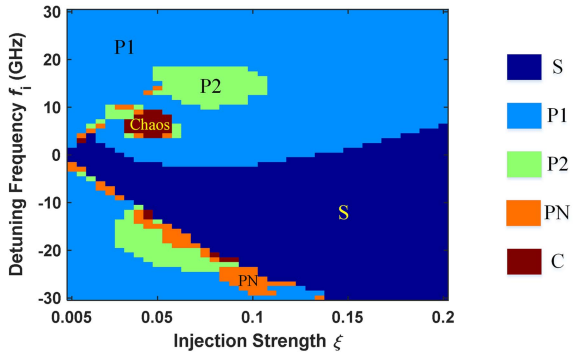

Fig. 2. Mappings of the nonlinear dynamic as a function of the injection strength ξ and the detuning frequency f_i. S: stable locking; P1: period-one oscillation; P2: period-two oscillation; PN: periods higher than two, which include period-three oscillation and period-four oscillation; C: chaos.

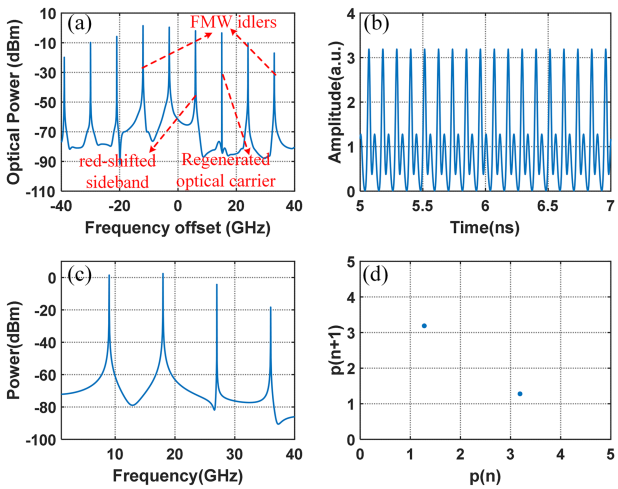

Fig. 3. Simulation results for P2 oscillation dynamics: (a) the optical spectrum, (b) the time domain waveform, (c) the electrical spectrum, and (d) the phase portrait when $f_i = 15$ GHz and $\xi = 0.08$.

relaxation resonance frequency f_r of the SL. It should also be noted that the region of P2 oscillation state is the second largest region among the periodic oscillations, and it occurs only in the relatively weak injection strength region.

To characterize the P2 oscillation properties, the numerically calculated optical spectrum, time-domain waveform, electrical spectrum, and phase portrait are plotted in Fig. 3. The detuning frequency is set as $f_i = 15$ GHz, and the injection strength is chose as $\xi = 0.08$. In Fig. 3(a), the regenerated optical carrier, red-shifted sidebands, and four-wave mixing (FWM) idlers are clearly observed. In addition, it is found that the frequency interval between sidebands in the optical spectrum is reduced to half that of P1 oscillation frequency. The time-domain waveform is shown in Fig. 3(b), of which the amplitude fluctuates alternately and has two peaks of intensity. After optical-to-electrical conversion, the subharmonic frequency at 9.01 GHz is generated and the corresponding electrical spectrum is shown in Fig. 3(c). The phase portrait of peak series is also plotted, where p(n) are consecutive peak intensity values in given time series. In Fig. 3(d), the phase portrait shows two clear dots, representing

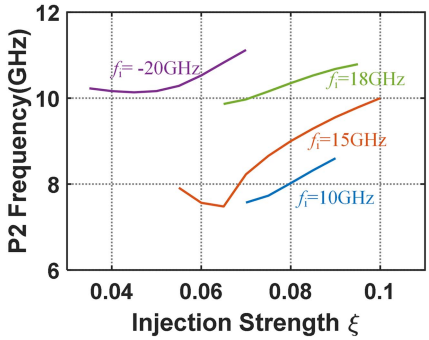

Fig. 4. Simulation results for the P2 oscillation frequency as a function of the injection strength ξ subject to different detuning frequencies.

the peak series repeat periodically every two pulses, which are typical characteristics of P2 oscillation.

Next, to validate the frequency tunability of P2 oscillation, the P2 oscillation frequency as a function of the injection strength ξ subject to different detuning frequencies are plotted in Fig. 4. According to the mappings of the nonlinear dynamics in Fig. 2, the detuning frequency is set as 10 GHz, 15 GHz, 18 GHz, and -20 GHz, respectively. It is observed that the P2 oscillation frequency increases nonlinearly with injection strength for different detuning frequencies. Especially, as indicated in Fig. 4, when the detuning frequency is set as $f_i = 15$ GHz, the P2 oscillation frequency decreases with injection strength ξ for $\xi < 0.065$ and increases abruptly for $\xi > 0.065$, which verify that the P2 oscillation is affected simultaneously by red-shifted effect and injection pulling effect as P1 oscillation [34]. Hereinto, the red-shift effect comes from the anti-guidance effect of the semiconductor laser, while the injection-pulling effect arises from the fact that the semiconductor laser is a detuned oscillator with its oscillation frequency pulled towards the injected frequency. Hence, the P2 oscillation frequency could be continuously tuned by properly changing the injection condition. Furthermore, it is observed that the P2 oscillation frequencies are below 12 GHz as the injection parameters changes, proving that the P2 oscillation can be used as a complement of P1 oscillation to generate low frequency microwave signals.

Furthermore, the frequency switching properties of P2 oscillation are investigated, which is important for generating SF microwave signals. To achieve frequency switching, the detuning frequency f_i is chosen as 15 GHz to excite P2 oscillation according the mappings of the nonlinear dynamics in Fig. 2. The injection strength of 0.064 and 0.096 are switched alternately with the repetition rate of 50 MHz, as depicted in Fig. 5(a). Fig. 5(b) shows the corresponding time-domain waveform of generated signal. The temporal period is 20 ns, which equals to that of the injection strength. Fig. 5(c) shows the detailed time-domain waveform. The amplitude has two peaks of intensity, indicating the P2 oscillation is excited. The interval between adjacent peaks is 0.13 ns and 0.1 ns under different injection strength, which corresponds to the P2 oscillation frequency of 7.48 GHz and 9.84 GHz, respectively. Fig. 5(d) shows the time-frequency diagram calculated by performing short-time Fourier transformation (STFT) to the time-domain waveform. It can

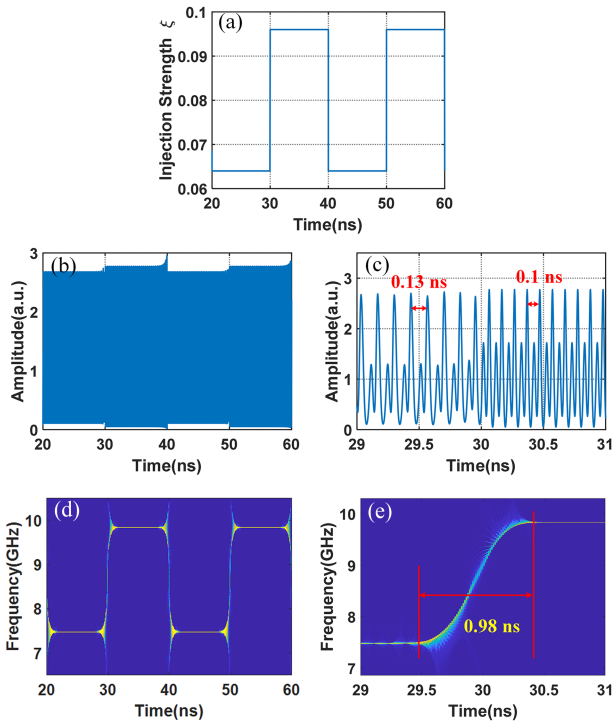

Fig. 5. Simulation results for the stepped-frequency signal generation based on P2 dynamics: (a) the injection strength, (b) the time domain waveform, and (c) the detailed time domain waveform, (d) the time-frequency diagram, (e) the detailed time-frequency diagram, where the injection strength ξ of 0.064 and 0.096 are switched alternately at fixed detuning frequency $f_i = 15$ GHz.

be found the instantaneous frequency switches periodically between 7.48 GHz and 9.84 GHz as the injection strength changes. To quantify the frequency-switching time, Fig. 5(e) shows the detailed time-frequency diagram. The frequency-switching time is measured as 0.98 ns, which is in nanosecond order. Thus, by fast tuning injection strength at fixed detuning frequency, the P2 oscillation dynamics can be used for the generation of high-speed microwave stepped-frequency or frequency-coding signals.

III. Experimental Demonstration

A. Single-Frequency Signal Generation

To verify the feasibility of the microwave signal generation system based on P2 dynamics, an experiment is implemented based on the setup in Fig. 1. The ML is a tunable narrow-linewidth laser (ID Photonics, CoBrite) of which the wavelength can be tuned from 1528.77 to 1563.86 nm. The SL is a distributed-feedback semiconductor laser (Micro Photons, PL-DFB-1550-C-A81-PA-14-BF).The bias current is set as 34 mA, about 5 times its threshold. The free-running output power and wavelength is 6.74 dBm and 1548.09 nm, respectively. When the wavelength of the ML is tuned to 1548 nm and the injected optical power is set as 1.66dBm, the optical spectra of the free-running SL and ML are measured using an optical spectrum analyzer (OSA, Yokogawa AQ6370D) with a wavelength resolution of 0.02 nm, as depicted in Fig. 6. In this case, the corresponding optical injection parameters are set to (f_i, ξ) = (11 GHz, 0.557). After optical injection, the optical spectrum measured at the output of the SL is shown in Fig. 6, in which the redshifted sideband, FWM idlers and regenerated optical carrier, are successfully generated. Then, the output signal of the SL is sent to a PD (Discovery, DSC40S) with a bandwidth of ~20 GHz to perform optical-to-electrical conversion.

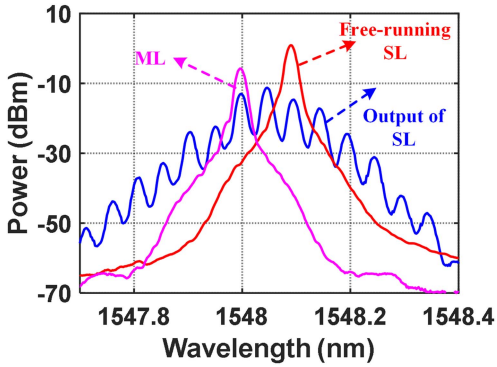

Fig. 6. The optical spectra of the injected ML (magenta line), the free-sunning SL (red line) and the output of SL after injection (blue line).

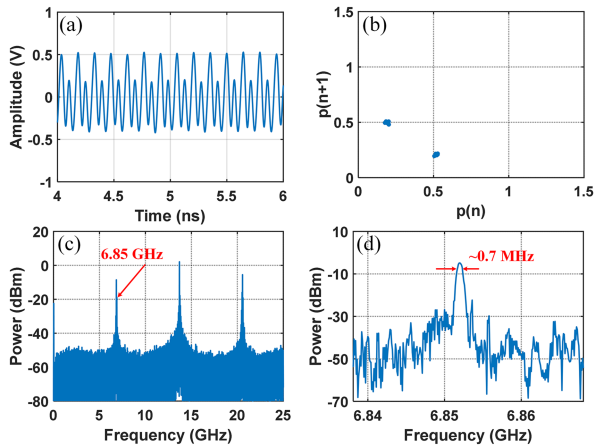

Fig. 7. The measured (a) time-domain waveform, (b) phase portrait, (c) electrical spectra with an observation span of 25 GHz and RBW of 100 kHz and (b) detailed electrical spectra with an observation span of 30 MHz and RBW of 510 kHz based on traditional optical injection.

Fig. 7(a) shows the time-domain waveform of the generated microwave signal, which is sampled by a real-time oscilloscope (OSC, Keysight DSO-X 92504A) with a sampling rate of 80 GSa/s. The amplitude has two peaks of intensity that fluctuate alternately. The phase portrait is measured and depicted in Fig. 7(b), which exhibits two clear dots. These results agree well with the above simulation results in Fig. 3 and verify that P2 oscillation is successfully excited. Moreover, the electrical spectrum is measured by an ESA (R&SRSWP-50) with a observation span of 25 GHz and resolution bandwidth (RBW) of 100 kHz, as shown in Fig. 7(c). The generated microwave signal by P2 oscillation has a frequency of 6.85 GHz. However, due to the exist of FWM idlers, high-frequency harmonics are also generated, which can be removed by simply using an electrical band-pass filter in practical application. Fig. 7(d) shows the detailed electrical spectrum of the generated signal around

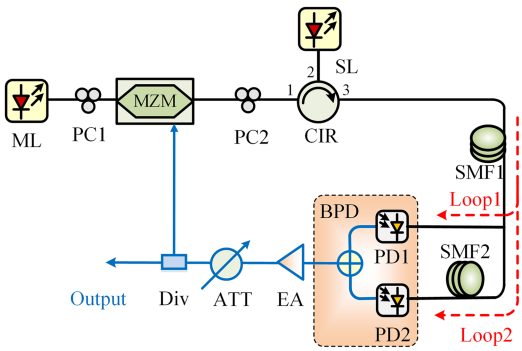

Fig. 8. Schematic diagram of the microwave signal generation system based on optically injected semiconductor laser combined optoelectronic feedback loop.

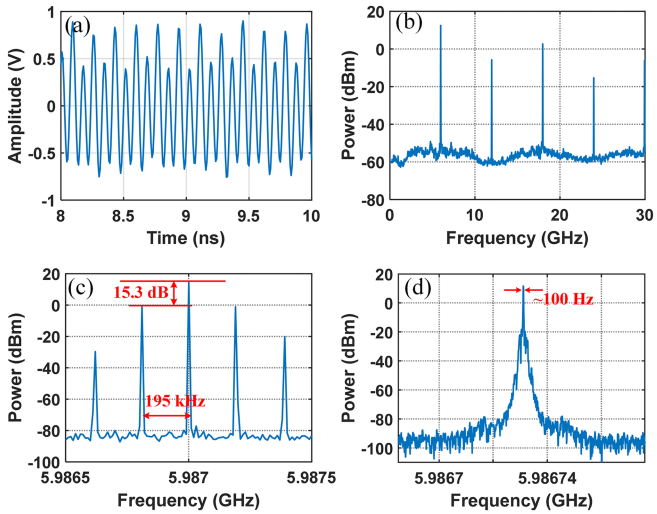

Fig. 9. (a) The time domain waveform, the electrical spectra (b) with an observation span of 30 GHz and RBW of 100 kHz, (c) with an observation span of 1 MHz and RBW of 300 Hz and (d) with an observation span of 100 kHz and RBW of 300 Hz of 5.987 GHz oscillation signal based on optoelectronic feedback single-loop.

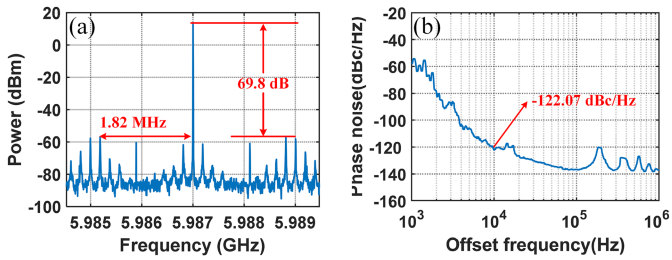

Fig. 10. (a) The electrical spectra with an observation span of 5 MHz and RBW of 300 Hz, (b) the measured phase noise of 5.987 GHz oscillation signal based on optoelectronic feedback dual-loop.

6.85 GHz when the RBW is 510 kHz and the span is set to 30 MHz. It is found that the generated signal has a large 3-dB spectral width of ∼0.7 MHz, which is mainly originated from the intrinsic semiconductor laser noise. To reduce the linewidth of the generated microwave signal, a dual-loop optoelectronic feedback structure is applied to the optical injection system, as shown in Fig. 8. In this system, the output of the SL after optical injection is transmitted through a span of single model fiber (SMF1, length: ∼1 km). The output signal is split into two branches, and the signal in one branch is delayed by another span of single mode fiber (SMF2, length: ∼500 m). Then, the signals in the two branches are sent to a balanced photodetector (BPD, FINISAR, BPDV2150R) to perform optical-to-electrical conversion. Afterwards, the obtained microwave signal is amplified by an electrical amplifier (EA, AT microwave, PA-0226-3827X, 2–l26 GHz) and attenuated by an electrical attenuator (ATT, Talent Microwave, TLVA0.1G-40G-40-10, 0.1-40 GHz) to adjust the feedback strength. The electrical signal is fed back to the modulator (MZM, Fujitsu, FTM7938EZ, Vπ: 3.5V) to form a closed loop. Here, the use of dual-loop optoelectronic feedback can effectively reduce the phase noise while suppressing the sidemodes [35], [36], [37].

As a comparison, the performance of using single-loop optoelectronic feedback structure (disconnecting the feedback loop2) is first investigated. By adjusting the ATT, the feedback power injected to the MZM is set as about −20 dBm. Fig. 9(a) shows the time-domain waveform of the generated single-frequency microwave signal. The amplitude has two peaks of intensity, which indicates P2 oscillation state is excited. Fig. 9(b) shows the measured spectrum of the generated microwave signal with an observation span of 30 GHz, in which the frequency of the generated signal is 5.987 GHz. Fig. 9(c) shows the detailed electrical spectrum when the RBW is 300 Hz and the observation span is set to 1 MHz. There are many sidemodes with frequency interval of 195 kHz, which is consistent with the theoretical free spectral range (FSR) determined by the loop length. The SMSR is measured to be 15.3 dB, which is related to the mode competition effect [37]. When the RBW and observation span is set as 300 Hz and 100 kHz respectively, the measured electrical spectrum is depicted in Fig. 9(d). It is observed that the 3-dB linewidth is below 100 Hz, which is obviously narrowed compared with that in Fig. 7. When dual-loop optoelectronic feedback is applied, Fig. 10(a) shows the electrical spectrum of the generated microwave signal when the RBW is 300 Hz and the observation span is set to 5 MHz. It is obvious that the SMSR reaches as high as 69.8 dB, which is markedly improved by 54.5 dB compared with that of the signal generated with single-loop feedback. Moreover, the phase noise of signal generated by dual-loop optoelectronic feedback P2 oscillation is also measured with the result shown in Fig. 10(b), in which the phase noise at 10 kHz frequency offset is −122.07 dBc/Hz.

Next, the frequency tuning property of P2 oscillation is investigated. In the experiment, the signal frequency is continuously tuned by changing the injected optical injection strength while fixing the detuning frequency. Fig. 11(a) shows the measured electrical spectra with different frequencies, including 1.72 GHz, 2.34 GHz, 3.54 GHz, 4.09 GHz, 4.77 GHz, 5.98 GHz, 7.44 GHz and 8.68 GHz. Fig. 11(b) shows the corresponding phase noise results of the generated single-frequency signals in which the phase noise is between −118.54 and −122.07 dBc/Hz at 10 kHz offset and between −134.20 and −139.42 dBc/Hz at 100 kHz

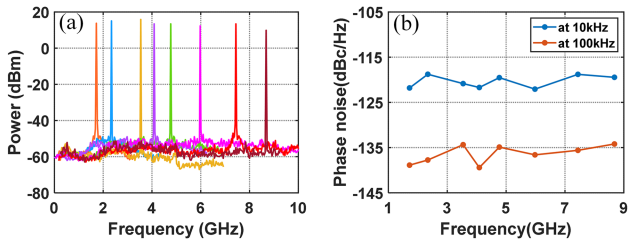

Fig. 11. (a) Measured electrical spectra and (b) phase noise when generating microwave signals from 1.72 GHz to 8.68 GHz.

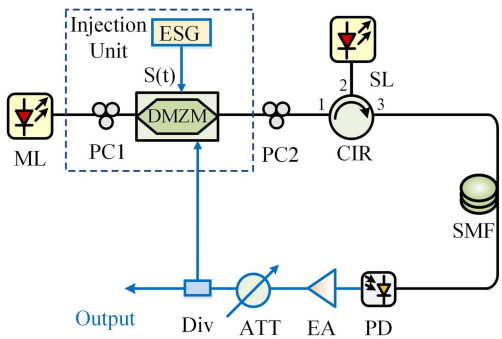

Fig. 12. Schematic diagram of the SF signal generation system based on optically injected semiconductor laser combined optoelectronic feedback.

offset, respectively. Therefore, by using P2 oscillation with optoelectronic feedback, high-quality single frequency microwave signals with tunable frequency are generated.

B. Stepped-Frequency Signal Generation

Using P2 dynamics, the generation of SF signal is implemented based on the setup in Fig. 12. An injection unit consisting of a low-speed electrical signal generator (ESG, RIGOL DG4062, 500 Msa/s), a polarization controller and a dual-drive Mach-Zehnder modulator (DMZM) is introduced to rapidly tune the optical injection strength. To this end, a control signal with properly programmed temporal period and amplitude is generated by the ESG. It is fed to one of the RF port of a DMZM (Fujitsu, FTM7937EZ) having a bandwidth of ∼25 GHz for intensity modulation, so that the injection strength varies periodically with the control signal. Accordingly, the P2 oscillation frequency is fast changed as the control signal varies. To check the feasibility of SF signal generation, the control signal is set to a 4-level signal with its amplitudes varies from −3.881 V to −3.796 V. The repetitive rate of this signal is 200 kHz and the corresponding temporal period is 5 μs, as depicted in Fig. 13(a). Fig. 13(b) shows the waveform of the generated SF signal in a single period of 5 μs. Fig. 13(c) shows the measured electrical spectrum in which four frequency lines at 3 GHz, 4 GHz, 5 GHz and 6 GHz are observed. Fig. 13(d) shows the time-frequency diagram of the generated signal that is obtained by performing STFT to the sampled waveform. It is clear that the signal has a stepped frequency profile covering four frequency components. It should be noted that, when the frequency jumps from 6 GHz to 3 GHz, obvious damping oscillation appears, resulting in

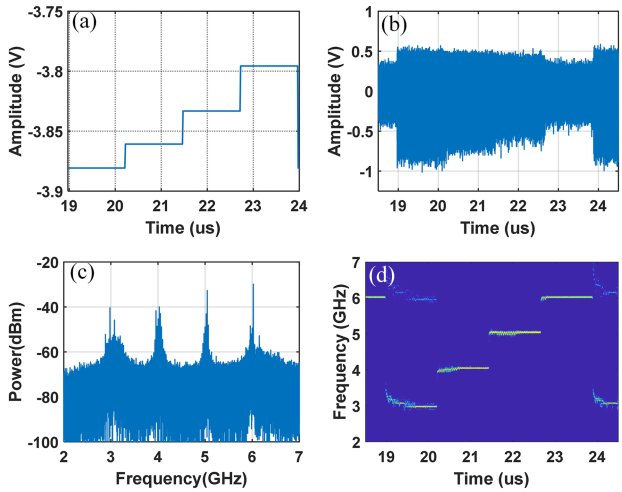

Fig. 13. (a) The specially designed step-level electrical control signal, (b) the time-domain waveform, (c) the electrical spectrum and (d) the recovered instantaneous frequency of the generated SF signal.

frequency jitter and linewidth broadening in the time-frequency diagram. This is caused by the semiconductor laser transient properties including the turn-on delay, relaxation oscillation and self-pulsation [38], and this inevitably deteriorates the frequency stability and accuracy. To address this problem, we introduce an optoelectronic feedback loop to the SF signal generation system. The mechanism of optoelectronic feedback loop for periodic signals is also called Fourier domain mode-locking (FDML), which is equivalent to a transient filter with a frequency interval of FSR and its frequency window varies with time [39], [40], [41], [42]. When the round-trip time delay of the optoelectronic feedback loop T_{loop} matches with the temporal period T of the generated periodic signal, i.e., $T_{loop} = N \times T$, in which N is a positive integer, stable FDML is achieved. In this case, the delayed signal through the feedback loop can be injected locking the existing oscillation, which breaking the limitation of mode building time [41]. In addition, the FDML produces a fixed phase relation between the longitudinal cavity modes such that the quality of the generated SF signal is improved [40].

In the experiment, the feedback loop is closed with a round-trip time delay of 5 μs. To meet the requirement of FDML, the control signal is also set to have a temporal period of 5 μs ($N = 1$) in Fig. 14(a). When the feedback power injected to the DMZM is adjusted to −22 dBm, stable FDML is achieved. The time-domain waveform of the generated signal is presented in Fig. 14(b), in which the temporal period is 5 μs. The measured electrical spectrum is depicted in Fig. 14(c) and the corresponding instantaneous frequency is presented in Fig. 14(d). It is observed the 3-dB linewidth of each spectral line is obviously narrowed and the damping oscillation is well suppressed compared with the results in Fig. 13, which verifies the benefits of the FDML-based P2 laser dynamics over the method without FDML.

Finally, the reconfigurability of SF signal generation by P2 laser dynamics is tested. By changing the electrical control signal to have a 13-level profile, the generation of 3-GHz bandwidth (3-6 GHz) SF signals having 13 discrete frequencies

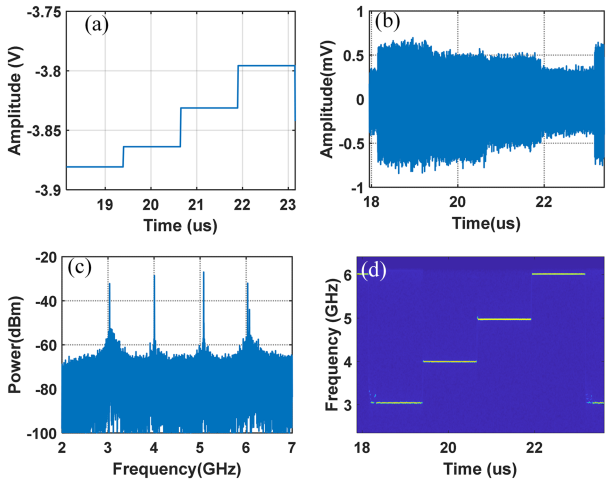

Fig. 14. (a) The specially designed step-level electrical control signal, (b) the time-domain waveform, (c) the electrical spectrum and (d) the recovered instantaneous frequency of the generated SF signal with FDML.

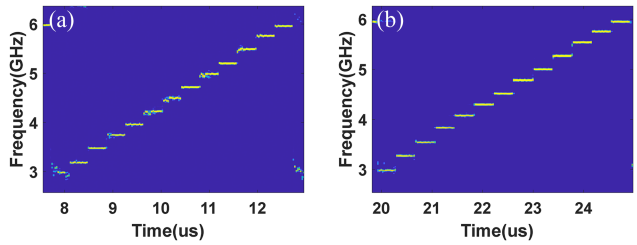

Fig. 15. The recovered instantaneous frequency when the frequency spacing is 250MHz (a) without FDML and (b) with FDML.

with an equal spacing of 250 MHz is realized. When FDML is not applied in the system, the time-frequency diagram of the generated SF signal is presented in Fig. 15(a). Obviously, the frequency damping oscillation still exist, deteriorating the frequency accuracy. When FDML is applied, the SF signal is improved with its time-frequency diagram shown in Fig. 15(b), in which the damping oscillation is well suppressed and the frequency accuracy is improved. These results not only validate the advantage of FDML once again, but also demonstrate the reconfigurability of signal generation by P2 laser dynamics.

IV. Conclusion

In conclusion, an approach to photonic generation of microwave signals by P2 dynamics of optically injected semiconductor laser is investigated, Firstly, the characteristics of P2 oscillation are numerically simulated and analyzed. The P2 oscillation frequency can be continuously tuned by changing the injection parameters and the additional frequency-switching time is in nanosecond order, which shows the potential of microwave signal generation by P2 dynamics. Next, the generation of single-frequency and SF microwave signals based on P2 dynamics are experimentally demonstrated. By incorporating a dual-loop optoelectronic feedback, single-frequency microwave signals with tunable frequencies from 1.72 GHz to 8.68 GHz is generated, of which the SMSR reaches 69.8 dB and the phase noise is below −118.54 dBc/Hz at 10 kHz offset and −134.20 dBc/Hz at 100 kHz offset. Besides, stepped-frequency signals with multiple discrete frequencies in the range from 3 GHz to 6 GHz are successfully generated, of which the bandwidth and frequency-step can be reconfigured. By further introducing a single-loop optoelectronic feedback loop, the frequency stability and accuracy are greatly improved. Therefore, the proposed approach based on P2 dynamics exhibits a feasible path toward a high-performance photonic-assisted microwave signals generation scheme, which may find applications in future sensing, communication, radar and signal processing.

References

[1] K. H. Lo, S. K. Hwang, and S. Donati, "Optical feedback stabilization of photonic microwave generation using period-one nonlinear dynamics of semiconductor lasers," *Opt. Exp.*, vol. 22, no. 15, pp. 18648–18661, Jul. 2014.

[2] J. Mørk, J. Mark, and B. Tromborg, "Route to chaos and competition between relaxation oscillations for a semiconductor laser with optical feedback," *Phys. Rev. Lett.*, vol. 65, pp. 1999–2002, Oct. 1990.

[3] J. Dong, J. Zhuang, and S. C. Chan, "Tunable switching between stable and periodic states in a semiconductor laser with feedback," *Opt. Lett.*, vol. 42, pp. 4291–4294, Oct. 2017.

[4] S. K. Hwang, J.-M. Liu, and J. K. White, "Characteristics of period-one oscillations in semiconductor lasers subject to optical injection," *IEEE J. Sel. Topics Quantum Electron.*, vol. 10, no. 5, pp. 974–981, Sep./Oct. 2004.

[5] T. Simpson, J. M. Liu, A. Gavrielides, V. Kovanis, and P. Alsing, "Period-doubling cascades and chaos in a semiconductor laser with optical injection," *Phys. Rev. A.*, vol. 51, no. 5, pp. 4181–4185, May 1995.

[6] T. Simpson, J. M. Liu, K. Huang, and K. Tai, "Nonlinear dynamics induced by external optical injection in semiconductor lasers," *Quantum Semiclassical Opt.*, vol. 9, pp. 765–784, May 1997.

[7] F. Lin and J. M. Liu, "Nonlinear dynamical characteristics of an optically injected semiconductor laser subject to optoelectronic feedback," *Opt. Commun.*, vol. 221, no. 1–3, pp. 173–180, Jun. 2003.

[8] R. Zhang, P. Zhou, K. Li, H. Bao, and N. Li, "Photonic generation of high-performance microwave frequency combs using an optically injected semiconductor laser with dual-loop optoelectronic feedback," *Opt. Lett.*, vol. 46, no. 18, pp. 4622–4625, Sep. 2021.

[9] J. S. Suelzer, T. B. Simpson, P. Devgan, and N. G. Usechak, "Tunable, low-phase-noise microwave signals from an optically injected semiconductor laser with opto-electronic feedback," *Opt. Lett.*, vol. 42, no. 16, pp. 3181–3184, Aug. 2017.

[10] T. B. Simpson, J. M. Liu, and A. Gavrielides, "Bandwidth enhancement and broadband noise reduction in injection-locked semiconductor lasers," *IEEE Photon. Technol. Lett.*, vol. 7, no. 7, pp. 709–711, Jul. 1995.

[11] Z. Liu and R. Slavík, "Optical injection locking: From principle to applications," *J. Lightw. Technol.*, vol. 38, no. 1, pp. 43–59, Jan. 2020.

[12] J. M. Liu, H. F. Chen, and S. Tang, "Optical-communication systems based on chaos in semiconductor lasers," *IEEE Trans. Circuits Syst. I: Fundam. Theory Appl.*, vol. 48, no. 12, pp. 1475–1483, Dec. 2001.

[13] S. Tang and J. M. Liu, "Chaos synchronized in semiconductor lasers with optoelectronic feedback," *IEEE J. Quantum Electron.*, vol. 39, no. 6, pp. 708–715, Jun. 2003.

[14] S. Tang and J. M. Liu, "Chaotic pulsing and quasiperiodic route to chaos in a semiconductor laser with delayed opto-electronic feedback," *IEEE J. Quantum Electron.*, vol. 37, no. 3, pp. 329–336, Mar. 2001.

[15] S. C. Chan, "Analysis of an optically injected semiconductor laser for microwave generation," *IEEE J. Quantum Electron.*, vol. 46, no. 3, pp. 421–428, Mar. 2010.

[16] X. Yu, F. Zhang, B. Wu, H. Dai, X. Li, and S. Pan, "Frequency-tunable microwave generation with parity–time symmetry period-one laser dynamics," *Opt. Lett.*, vol. 48, no. 6, pp. 1355–1358, Mar. 2023.

[17] X.-Q. Qi and J.-M. Liu, "Photonic microwave applications of the dynamics of semiconductor lasers," *IEEE J. Sel. Topics Quantum Electron.*, vol. 17, no. 5, pp. 1198–1211, Sep./Oct. 2011.

[18] X. Yu, F. Zhang, B. Wu, G. Sun, S. Pan, and X. Li, "Reconfigurable frequency-modulated microwave generation using multi-wavelength optically injected semiconductor laser," in *Proc. 2023 Opto-Electron. Commun. Conf.*, Jul. 2023, pp. 1–4.

[19] E. K. Lau, X. Zhao, H. K. Sung, D. Parekh, C. C. Hasnain, and M. Wu, "Strong optical injection-locked semiconductor lasers demonstrating >100-GHz resonance frequencies and 80-GHz intrinsic bandwidths," *Opt. Exp.*, vol. 16, no. 9, pp. 6609–6618, Apr. 2008.

[20] P. Zhou, F. Zhang, Q. Guo, S. Li, and S. Pan, "Reconfigurable radar waveform generation based on an optically injected semiconductor laser," *IEEE J. Sel. Topics Quantum Electron.*, vol. 23, no. 6, Nov./Dec. 2017, Art. no. 1801109.

[21] P. Zhou et al., "Generation of NLFM microwave waveforms based on controlled period-one dynamics of semiconductor lasers," *Opt. Exp.*, vol. 28, pp. 32647–32656, Oct. 2020.

[22] S. C. Chan, S. K. Hwang, and J. Liu, "Period-one oscillation for photonic microwave transmission using an optically injected semiconductor laser," *Opt. Exp.*, vol. 15, pp. 14921–14935, Oct. 2007.

[23] X. Yu, G. Sun, F. Zhang, and S. Pan, "Frequency-modulated microwave signal generation by dual-wavelength-injection period-one laser dynamics," *Opt. Lett.*, vol. 47, no. 22, pp. 5921–5924, Nov. 2022.

[24] X. Yu, F. Zhang, G. Sun, B. Wu, S. Pan, and Y. Zhou, "Frequency-modulated microwave signal generation by dual-wavelength optically injected semiconductor laser," in *Proc. 2022 IEEE Int. Topical Meeting Microw. Photon.*, Orlando, FL, USA, Oct. 2022, pp. 1–4.

[25] G. Sun, Y. Zhou, Y. He, X. Yu, F. Zhang, and S. Pan, "Photonics-based MIMO radar with broadband digital coincidence imaging," *IEEE Trans. Microw. Theory Techn.*, vol. 72, no. 12, pp. 6996–7003, Dec. 2024.

[26] G. Sun et al., "Photonics-based broadband single-input-multiple- output-OAM coincidence imaging," *IEEE Trans. Radar Syst.*, vol. 2, pp. 690–698, 2024.

[27] B. Wu, F. Zhang, X. Yu, X. Wang, S. Pan, and X. Li, "Stepped frequency radar with broadband signal generation by period one laser dynamics," in *Proc. 2023 Asia Commun. Photon. Conf./2023 Int. Photon. Optoelectron. Meetings*., Wuhan, China, Nov. 2023, pp. 1–4.

[28] X. Yu et al., "Frequency-tunable narrow linewidth THz signal generation by semiconductor lasers subject to mutual optical injection," in *Proc. 2023 Asia Commun. Photon. Conf./2023 Int. Photon. Optoelectron. Meetings*, Wuhan, China, Nov. 2023, pp. 1–3.

[29] E. A. Kittlaus et al., "A low-noise photonic heterodyne synthesizer and its application to millimeter-wave radar," *Nature Commun.*, vol. 12, no. 1, , Jul. 2021, Art. no. 4397.

[30] S. K. Hwang, J. M. Liu, and J. K. White, "35-GHz intrinsic bandwidth for direct modulation in 1.3 μm semiconductor lasers subject to strong injection locking," *IEEE Photon. Technol. Lett.*, vol. 16, no. 4, pp. 972–974, Apr. 2004.

[31] S. Cundiff and A. M. Weiner, "Optical arbitrary waveform generation," *Nature Photon.*, vol. 4, pp. 760–766, Oct. 2010.

[32] A. Rashidinejad and A. M. Weiner, "Photonic radio-frequency arbitrary waveform generation with maximal time-bandwidth product capability," *J. Lightw. Technol.*, vol. 32, no. 20, pp. 3383–3393, Oct. 2014.

[33] S. C. Chan and J. M. Liu, "Microwave frequency division and multiplication using an optically injected semiconductor laser," *IEEE J. Quantum Electron.*, vol. 41, no. 9, pp. 1142–1147, Aug. 2005.

[34] T. B. Simpson, J. M. Liu, M. A. Almulla, N. G. Usechak, and V. Kovanis, "Limit-cycle dynamics with reduced sensitivity to perturbations," *Phys. Rev. Lett.*, vol. 112, no. 2, Jan. 2014, Art. no. 023901.

[35] X. S. Yao and L. Maleki, "Multiloop optoelectronic oscillator," *IEEE J.Quantum Electron.*, vol. 36, no. 1, pp. 79–84, Jan. 2000.

[36] P. Zhou, F. Zhang, D. Zhang, and S. Pan, "Performance enhancement of an optically-injected-semiconductor-laser-based optoelectronic oscillator by subharmonic microwave modulation," *Opt. Lett.*, vol. 43, no. 21, pp. 5439–5442, Oct. 2018.

[37] P. Hao, J. Niu, X. Wang, and X. S. Yao, "Dual-loop diode-tuned Fourier domain harmonically mode-locked opto-electronic oscillator with over 50 dB side-mode spur reduction," *Opt. Exp.*, vol. 30, no. 25, pp. 45569–45582, Nov. 2022.

[38] G. Arnold and P. Russer, "Modulation behavior of semiconductor injection lasers," *Appl. Phys.*, vol. 14, pp. 255–268, Nov. 1977.

[39] J. Zhuang, X. Li, S. Li, and S. C. Chan, "Frequency-modulated microwave generation with feedback stabilization using an optically injected semiconductor laser," *Opt. Lett.*, vol. 41, no. 24, pp. 5764–5767, Dec. 2016.

[40] R. Huber, M. Wojtkowski, and J. G. Fujimoto, "Fourier domain mode locking (FDML): A new laser operating regime and applications for optical coherence tomography," *Opt. Exp.*, vol. 14, no. 8, pp. 3225–3237, Apr. 2006.

[41] T. Hao et al., "Breaking the limitation of mode building time in an optoelectronic oscillator," *Nature Commun.*, vol. 9, May 2018, Art. no. 1839.

[42] X. Yu et al., "Broadband stepped-frequency radar waveform generation by fourier domain mode-locking period-one laser dynamics," *Opt. Lett.*, vol. 49, no. 15, pp. 4266–4269, Jul. 2024.